

Reconfigurable Intelligent Surface-Based Receive Generalized Spatial Modulation Design

Xinghao Guo*, Hanjiang Hong*, Yin Xu*, Yi-yan Wu[†], Dazhi He* and Wenjun Zhang*

* School of Electronic Information and Electrical Engineering, Shanghai Jiao Tong University, Shanghai 200240, China

Email: {guoxinghao, honghj, xuyin, hedazhi, zhangwenjun}@sjtu.edu.cn

[†] Wireless Technology Research Department, Communications Research Centre, Ottawa ON K2K 2Y6, Canada

Email: yiyan.wu@ieee.org

Abstract—In this paper, the receive generalized spatial modulation (RGSM) scheme with reconfigurable intelligent surfaces (RIS) assistance is proposed. The RIS group controllers change the reflected phases of the RIS elements to achieve the selection of receive antennas and phase shift keying (PSK) modulation, and the amplitudes of the received symbols are adjusted by changing the activation states of the elements to achieve amplitude phase shift keying (APSK) modulation. Compared with the existing RIS-aided receive generalized space shift keying (RIS-RGSSK) scheme, the proposed scheme realizes that the selected antennas respectively receive different modulation symbols, and only adds the process to control the modulated phases and the activation states of elements. The proposed scheme has better bit error rate (BER) performance than the RIS-RGSSK scheme at the same rate. In addition, the results show that for low modulation orders, the proposed scheme will perform better with PSK, while for high modulation order, APSK is better. The proposed scheme is a promising scheme for future wireless communication to achieve high-efficiency.

Index Terms—RGSM, RIS, space shift keying, receive spatial modulation, APSK.

I. INTRODUCTION

WITH the massive growth of mobile devices and the widespread application of the Internet of Things (IoT), the future wireless communication is expected to achieve higher data transmission rates, spectral efficiency, and energy efficiency. There are various solutions in the physical layer to improve the efficiency and reliability, e.g., non-orthogonal multiple access (NOMA) [1]–[3], massive multiple-input-multiple-output (MIMO) [4], [5], reconfigurable intelligent surfaces (RIS) [6], [7], etc.

Spatial modulation (SM) is a promising MIMO transmission technology that uses the indices of the active antenna to convey additional spatial bits [8]. SM can achieve high transmission capacity and reduce Inter-Antenna-Synchronization (IAS) requirements and Inter Antenna Interference (IAI) [9], [10]. Due to the advantages mentioned above, SM has become a hot spot in the MIMO research field. Subsequently, the fundamental SM and space shift keying (SSK) were extended to many variants for spectral efficiency, such as generalized space shift keying (GSSK) [11], generalized spatial modulation (GSM) [12], and receive spatial modulation (RSM) [13].

RIS consists of many low-cost and energy-efficient passive reflective elements, which can control the scattering and propagation of the incident wave in the channel by inducing a pre-designed phase shift. In particular, [14] innovatively proposed the the RIS-aided RSSK (RIS-RSSK) and RSM (RIS-RSM) schemes, in which RIS-access point (RIS-AP) was adopted. RIS forms part of the transmitter and compensates for the phases of the channel to realize the selection of the receive antennas. The numerical results demonstrate the superiority of the RIS-aided schemes. Then, the combination of RIS and SM becomes a popular direction to work on. In [15], an RIS-SSK scheme with multiple transmit antennas is proposed, where the spatial information bits are mapped to the indices of the transmit antennas and the RIS reflects the signal to the single-antenna receiver. In order to obtain additional spectral efficiency, an RIS-SM scheme that uses the indices of both the transmit and receive antennas to convey spatial bits was proposed in [16]. However, the results showed that the error probability of the bits used to select the transmit antennas is significantly lower than those used to select the receive antennas. SM is also applied to the RIS entity to transmit additional bits through RIS element groups [17].

At the same time, inspired by [14], RIS-assisted RSM schemes have been further developed. In order to simultaneously target two receive antennas, the RIS-assisted receive quadrature space-shift keying (RIS-RQSSK) is proposed in [18]. The authors then proposed the RIS-assisted receive quadrature spatial modulation (RIS-RQSM) scheme to achieve higher spectral efficiency [19]. Nevertheless, in the above RSM scheme, the data rate grows logarithmically rather than linearly with the number of receive antennas, and the restriction that the number of receive antennas equals the power of two needs to be satisfied. As a natural extension of RIS-SSK, the RIS-aided receive generalized space shift keying (RIS-RGSSK) was proposed in [20]. To the best of our knowledge, none of the existing studies consider the combination of RIS and GSM in RSM scheme. The reason is mainly that under the RSM schemes, the modulated symbols at the transmitter cannot achieve diversity at different selected receive antennas.

To fill this gap, RIS-aided receive generalized spatial modulation (RIS-RGSM) scheme is proposed in this paper. Com-

pared with the RIS-RGSSK scheme, the RIS group controllers only require the control process for modulation phases and activation states of elements, which brings a significant increase in transmission rate and performance gain.

The rest of this paper is organized as follows: Section II introduces the RIS-RGSM system model and the realization principle of the selected antennas receiving different modulation symbols. Section III analyzes the theoretical performance of the proposed system. Section IV shows the simulation and comparison results, and conducts the correlation analysis. Section V concludes the paper.

Notation: Bold, lowercase and capital letters are used for vectors and matrices. $\mathbf{A}_{m \times n}$ denote the matrix \mathbf{A} with m rows and n columns, where $\mathbf{A}_{i,j}$ denotes the element in row i and column j , and $\mathbf{A}_{i,:}$ denotes the i -th row of matrix \mathbf{A} . $()^T$ and $()^H$ denote transposition and Hermitian transposition, respectively. The real and imaginary parts of a complex variable X are denoted by $\Re\{X\}$ and $\Im\{X\}$, respectively. $f_X(x)$ and $M_X(x)$ respectively stand for the probability density function and moment generating function of a random variable (RV) X . $Q(\cdot)$ is the Gaussian Q -function and $j = \sqrt{-1}$.

II. SYSTEM MODEL

The proposed RIS-RGSM system is shown in Fig. 1, where the transmitter has one antenna, the receiver has N_R antennas, and N_a active antennas are selected to convey the spatial information bits. A barrier blocks the line-of-sight (LOS) path between the transmitter and the receiver. In addition, the RIS with N elements works in the RIS access point (RIS-AP) mode¹, that is, as part of the transmitter to reflect the signals to the receiver [21], [22], and the path loss and scattering of the link between the RIS and the transmit antenna is negligible².

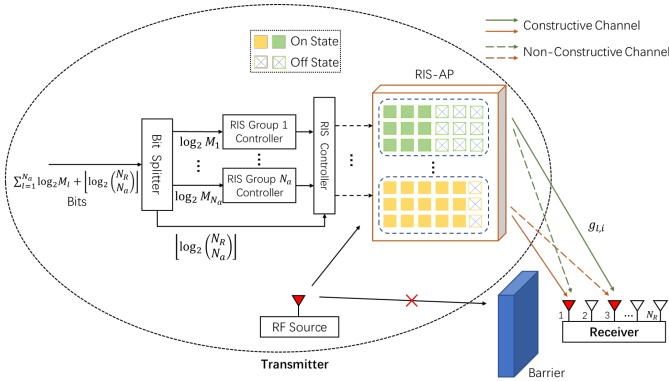


Fig. 1: Diagram of the RIS-RGSM system.

¹Note that the proposed system could alternatively be implemented using conventional analog beamforming. Nevertheless, the benefits offered by RISs, including near-passive operation, capacity to enable full-duplex communication with minimal self-interference, and independence from feeding networks, strongly motivate us to incorporate this state-of-the-art technology into the proposed system.

²Due to the short distance, there is a strong line-of-sight (LOS) component, which is generally stronger and more stable than the other components of the wireless channel subject to random scattering and reflection. The strong LoS component makes the wireless channel less random and more deterministic.

GSM works at the receiver, which maps the spatial bits into the indices of N_a selected antennas with the condition of $N_a \ll N_R$. The number of permutation combinations of N_a selected from N_R antennas is $C_{N_R}^{N_a}$. According to the working principle of GSM, the number of selected antennas combinations must be a power of two [12]. Therefore, $N_c = 2^{m_0}$ combinations need to be selected out of all combinations, where m_0 is the number of bits represented by one antennas combination and given by $m_0 = \lceil \log_2 \binom{N_R}{N_a} \rceil$.

The information bits are sent to the RIS controller, which will then adjust the phases of the reflected signal based on the input bits and the knowledge of channel phases. RIS elements are divided into N_a groups with $N_g = \frac{N}{N_a}$ elements. The l -th group is controlled to adjust the reflected signal phase $\phi_{l,(l-1)N_g+1:lN_g}$ to specifically maximize the signal-to-noise ratio (SNR) at the l -th active receive antenna, where $l \in \{1, 2, \dots, N_a\}$. For simplicity, a matrix $\Phi_{N_a \times N_g}$ is used to store the reflected phases of the RIS elements, where the l -th row $\Phi_{l,:} = \phi_{l,(l-1)N_g+1:lN_g}$.

A. Transmission

The wireless channel between the i -th reflected element of the RIS and the l -th receive antenna of the receiver is characterized by $g_{l,i} = \beta_{l,i} e^{-j\psi_{l,i}}$, where $i = 1, 2, \dots, N$, and follows a $\mathcal{CN}(0, 1)$ distribution under the assumption of flat Rayleigh fading channels. The received signal of the l -th selected antenna can be expressed as:

$$y_l = \sqrt{E_s} \left(\sum_{i=1}^{N_a} \sum_{k=1}^{N_g} g_{l,(i-1)N_g+k} e^{j\Phi_{i,k}} \right) + n_l \quad (1)$$

where E_s is the transmitted signal energy of the unmodulated carrier and n_l is the additive white Gaussian noise (AWGN) at the l -th receive antenna with zero mean and variance N_0 .

1) *RIS-RGSSK:* For RIS-RGSSK in [20], if the l -th antenna exists in the antennas combination selected by the m_0 bits, then the reflected phases of the N_g elements of the l -th RIS group satisfies $\Phi_{l,:} = \psi_{l,(l-1)N_g+1:lN_g}$, assuming the RIS has the knowledge of channel phases. Substituting the reflected phases into (1) yields the following:

$$y_l = \sqrt{E_s} \left(\sum_{k=1}^{N_g} \beta_{l,(l-1)N_g+k} + \sum_{i=1, i \neq l}^{N_a} \sum_{k=1}^{N_g} g_{l,(i-1)N_g+k} e^{j\Phi_{i,k}} \right) + n_l \quad (2)$$

According to (2), it can be found that the received signal of the l -th selected antenna is divided into two parts, one part is constructive after the N_g elements of the l -th RIS group specially adjust the phases for it to eliminate the channel phases, and the other part is the signals reflected from the elements of other groups, which is non-constructive and can be regarded as interference. Hence, the SNRs of the selected N_a antennas at the receiver can be maximized.

In the RIS-RGSSK system, the rate is $R = m_0$ bits per channel use (bpcu). In order to increase the rate, the transmit antenna can send the modulated symbol, but it can be found that the rate can only increase $\log_2 M$ when the modulation order is M , because there is only one transmit antenna and the selected N_a receive antennas will receive the same symbol.

2) *proposed RIS-RGSM with phase shift keying (PSK)*:

In order to increase the diversity and realize receive GSM (RGSM), this paper first proposed the RIS-RGSM scheme combined with the PSK modulation. In this scheme, the difference is that the transmit antenna only plays the role of excitation, while the transmit symbols are embodied by controlling the RIS elements. Note that in RIS-RGSSK, the l -th RIS group needs to eliminate the channel phases $\psi_{l,(l-1)N_g+1:lN_g}$. Since the phases should be changed according to the selected receive antenna, the additional phases, which can be controlled by the information bits, can be induced to modulate the phases of the reflected signals. Then, at the l -th selected antenna, it is equivalent to receiving the PSK symbols.

Therefore, as shown in Fig. 1, each RIS group is correspondingly equipped with a RIS group controller, which independently obtains an additional phase ϕ_l based on the input $m_l = \log_2 M_l$ information bits, where M_l is the received constellation order for the l -th selected antenna and $\phi_l \in \{0, \frac{2\pi}{M_l}, \dots, \frac{2\pi(M_l-1)}{M_l}\}$. The phase ϕ_l is then added with the channel phases $\psi_{l,(l-1)N_g+1:lN_g}$ that originally needs to be eliminated, so the reflected phases of the l -th RIS group is given by

$$\Phi_{l,:} = \psi_{l,(l-1)N_g+1:lN_g} + \phi_l \quad (3)$$

The received signal changes to:

$$y_l = \sqrt{E_s} \left(\sum_{k=1}^{N_g} \beta_{l,(l-1)N_g+k} e^{j\phi_l} + \sum_{i=1, i \neq l}^{N_a} \sum_{k=1}^{N_g} g_{l,(i-1)N_g+k} e^{j\Phi_{i,k}} \right) + n_l \quad (4)$$

So the rate is

$$R = \sum_{l=1}^{N_a} m_l + m_0 \quad \text{bpcu} \quad (5)$$

3) *proposed RIS-RGSM with amplitude phase shift keying (APSK)*: When the modulation order M_l becomes large, the minimum Euclidean distance of the PSK constellation decreases sharply, and the performance degrades, so the RIS-RGSM scheme with APSK is also proposed in this paper. For APSK with modulation order $M = M_r M_p$ using Gray mapping, constellation symbols are scattered on M_r concentric rings with uniformly increasing radius and each ring contains M_p uniform-distributed constellation symbols. In order to control the amplitude of the received symbols, the RIS group controller changes the number of activated elements (ON state) within the group according to the input $\log_2 M_r$ bits. For simplicity, the activation states of the RIS elements is represented by a matrix $\mathbf{F}_{N_a \times N_g}$ consisting of 0 and 1, and the l -th row $\mathbf{F}_{l,:}$ represents the active states of the l -th RIS

group. The number of 1s in the array $\mathbf{F}_{l,:}$ is in the range $\{\frac{N_g}{M_r}, \frac{2N_g}{M_r}, \dots, N_g\}$. The received signal is given by

$$y_l = \sqrt{E_s} \left(\sum_{k=1}^{N_g} \beta_{l,(l-1)N_g+k} \mathbf{F}_{l,k} e^{j\phi_l} + \sum_{i=1, i \neq l}^{N_a} \sum_{k=1}^{N_g} g_{l,(i-1)N_g+k} \mathbf{F}_{i,k} e^{j\Phi_{i,k}} \right) + n_l \quad (6)$$

where $\mathbf{F}_{i,k} = 1$ or 0, and $\phi_l \in \{0, \frac{2\pi}{M_p}, \dots, \frac{2\pi(M_p-1)}{M_p}\}$. When $\frac{N_g}{M_r} \gg 1$, applying the Central Limit Theorem (CLT), the transmitted symbol can be approximated by

$$s = \sqrt{E_s} \rho e^{j\phi} \quad (7)$$

where $\rho \in \{\frac{1}{M_r}, \frac{2}{M_r}, \dots, 1\}$, $\phi \in \{0, \frac{2\pi}{M_p}, \dots, \frac{2\pi(M_p-1)}{M_p}\}$, and the received signal can be approximated by

$$y_l = \sum_{k=1}^{N_g} \beta_{l,(l-1)N_g+k} s_l + \sum_{i=1, i \neq l}^{N_a} \sum_{k=1}^{N_g} g_{l,(i-1)N_g+k} e^{j\psi_{i,(i-1)N_g+k}} s_i + n_l \quad (8)$$

B. Detection

For detection, assuming the receiver has complete channel knowledge, the principle with the Maximum Likelihood (ML) detection can be expressed as:

$$\begin{aligned} (\hat{c}, \hat{\mathbf{s}}) &= \arg \min_{c, \mathbf{s}} \left| \sum_{l=1}^{N_a} \left(y_l - \sum_{i=1}^{N_a} \sum_{k=1}^{N_g} g_{l,(i-1)N_g+k} e^{j\psi_{i,(i-1)N_g+k}} s_i \right) \right|^2 \\ &= \arg \min_{c, \mathbf{s}} \left| \sum_{l=1}^{N_a} y_l - \sum_{l=1}^{N_a} \sum_{i=1}^{N_a} \sum_{k=1}^{N_g} g_{l,(i-1)N_g+k} e^{j\psi_{l,(i-1)N_g+k}} s_l \right|^2 \\ &= \arg \min_{c, \mathbf{s}} \left| y - \sum_{l=1}^{N_a} G_l s_l \right|^2 \\ &= \arg \min_{c, \mathbf{s}} |y - \mathbf{G} \cdot \mathbf{s}|^2 \end{aligned} \quad (9)$$

where $y = \sum_{l=1}^{N_a} y_l$ contains the received signal from all selected antennas, c denotes one combination from the N_c antennas combinations, so l is chosen from the N_a selected antennas contained within the combination c . The row vector $\mathbf{G} = [G_1, G_2, \dots, G_{N_a}]$ contains N_a coefficients, determined by the chosen antennas combination c , with $G_l = \sum_{i=1}^{N_a} \sum_{k=1}^{N_g} g_{l,(i-1)N_g+k} e^{j\psi_{l,(i-1)N_g+k}}$. The column vector $\mathbf{s} = [s_1, s_2, \dots, s_{N_a}]^T$ contains N_a symbols, which are received by each of the N_a selected antennas.

III. PERFORMANCE ANALYSIS

In this section, the theoretical bit error rate (BER) of the proposed RIS-RGSM system is analyzed based on the derivations in [14], [20]. From (9), conditioned on channel coefficients, the pairwise error probability (PEP) can be expressed as:

$$\begin{aligned} &P(c, \mathbf{s} \rightarrow \hat{c}, \hat{\mathbf{s}}) \\ &= P(|y - \mathbf{G}\mathbf{s}|^2 > |y - \hat{\mathbf{G}}\hat{\mathbf{s}}|^2) \\ &= P\left(-|\mathbf{G}\mathbf{s} - \hat{\mathbf{G}}\hat{\mathbf{s}}|^2 - 2\Re\left\{\sum_{l=1}^{N_a} n_l^* (\mathbf{G}\mathbf{s} - \hat{\mathbf{G}}\hat{\mathbf{s}})\right\} > 0\right) \\ &= P(D > 0) \end{aligned} \quad (10)$$

where $\Re\{x\}$ denotes the real part of a complex variable x . Here, $D \sim \mathcal{N}(\mu_D, \sigma_D^2)$ with $\mu_D = -|\mathbf{G}\mathbf{s} - \hat{\mathbf{G}}\hat{\mathbf{s}}|^2$ and $\sigma_D^2 = 2N_a N_0 |\mathbf{G}\mathbf{s} - \hat{\mathbf{G}}\hat{\mathbf{s}}|^2$. Therefore, from $P(D > 0) = Q(-\mu_D/\sigma_D)$, it follows that

$$P(c, \mathbf{s} \rightarrow \hat{c}, \hat{\mathbf{s}}) = Q\left(\sqrt{\frac{|\mathbf{G}\mathbf{s} - \hat{\mathbf{G}}\hat{\mathbf{s}}|^2}{2N_a N_0}}\right) \quad (11)$$

Defining $B = \mathbf{G}\mathbf{s} - \hat{\mathbf{G}}\hat{\mathbf{s}}$, which can be extended as:

$$\begin{aligned} B &= \mathbf{G}\mathbf{s} - \hat{\mathbf{G}}\hat{\mathbf{s}} \\ &= \sum_{l=1}^{N_a} \left(\sum_{k=1}^{N_g} \beta_{l,(l-1)N_g+k} s_l + \sum_{i=1, i \neq l}^{N_a} \sum_{k=1}^{N_g} g_{l,(i-1)N_g+k} e^{j\psi_{i,(i-1)N_g+k}} s_i \right. \\ &\quad \left. - \sum_{i=1}^{N_a} \sum_{k=1}^{N_g} \hat{g}_{l,(i-1)N_g+k} e^{j\psi_{i,(i-1)N_g+k}} \hat{s}_i \right) \end{aligned} \quad (12)$$

Here, we have $E[\beta] = \frac{\sqrt{\pi}}{2}$, $Var[\beta] = \frac{4-\pi}{4}$, $E[ge^{j\psi}] = 0$, and $Var[ge^{j\psi}] = 1$ [14]. Thus, applying the CLT, B follows the Gaussian distribution with the mean value $\mu_B = \frac{N_g \sqrt{\pi}}{2} \sum_{l=1}^{N_a} s_l$ and variance $\sigma_B^2 = (N - \frac{N_g \pi}{4}) \sum_{l=1}^{N_a} s_l + N \sum_{l=1}^{N_a} \hat{s}_l$. Let $\Gamma = B^2$, then Γ follows a non-central χ^2 distribution with one degree of freedom [20]. The PEP can be extended as:

$$\begin{aligned} \bar{P}(c, \mathbf{s} \rightarrow \hat{c}, \hat{\mathbf{s}}) &= \int_0^\infty Q\left(\sqrt{\frac{\Gamma}{2N_a N_0}}\right) f_\Gamma(\Gamma) d\Gamma \\ &= \frac{1}{\pi} \int_0^{\pi/2} M_\Gamma\left(\frac{-1}{4N_a N_0 \sin^2 \eta}\right) d\eta \end{aligned} \quad (13)$$

where $M_\Gamma(x)$ is the moment generating function (MGF) of Γ [14], which can be defined as

$$M_\Gamma(x) = \left(\frac{1}{\sqrt{1-2\sigma_B^2 x}}\right) \exp\left(\frac{\mu_B^2 x}{1-2\sigma_B^2 x}\right) \quad (14)$$

Besides, when $\sin^2 \eta = 1$, $M_\Gamma(x)$ can reach the upper bound, then substituting μ_B , σ_B^2 and this MGF in (13) provides the upper bound of PEP:

$$\begin{aligned} \bar{P}(c, \mathbf{s} \rightarrow \hat{c}, \hat{\mathbf{s}}) &\leq \frac{1}{2\sqrt{1 + \frac{(4N - N_g \pi) \sum_{l=1}^{N_a} s_l + 4N \sum_{l=1}^{N_a} \hat{s}_l}{16N_a N_0}}} e^{\left(\frac{-\frac{N_g^2 \pi^2 \sum_{l=1}^{N_a} s_l}{16N_a N_0}}{1 + \frac{(4N - N_g \pi) \sum_{l=1}^{N_a} s_l + 4N \sum_{l=1}^{N_a} \hat{s}_l}{16N_a N_0}}\right)} \end{aligned} \quad (15)$$

Finally, the average BER can be derived as:

$$P_b \leq \frac{1}{N_c \prod_{l=1}^{N_a} M_l} \sum_c \sum_s \sum_{\hat{c}} \sum_{\hat{s}} \frac{\bar{P}(c, \mathbf{s} \rightarrow \hat{c}, \hat{\mathbf{s}}) e(c, \mathbf{s} \rightarrow \hat{c}, \hat{\mathbf{s}})}{\sum_{l=1}^{N_a} M_l + m_0} \quad (16)$$

where $e(c, \mathbf{s} \rightarrow \hat{c}, \hat{\mathbf{s}})$ represents the number of bits in error for the corresponding pairwise error event [14].

IV. SIMULATION RESULTS

This section evaluates the proposed RIS-RGSM system performance and makes some comparisons. Both the receiver and RIS controllers have complete knowledge of the Rayleigh

channel. The large-scale path loss is not considered since it is implicitly taken into account in the received SNR. Besides, although the proposed scheme can realize that different selected antennas receive symbols with different modulation orders, for brevity, the modulation orders of N_a selected antennas are the same, that is, $M = M_1 = M_2 = \dots = M_{N_a}$. For fairness and comparison purposes, E_s is assumed to be 1 in the simulation.

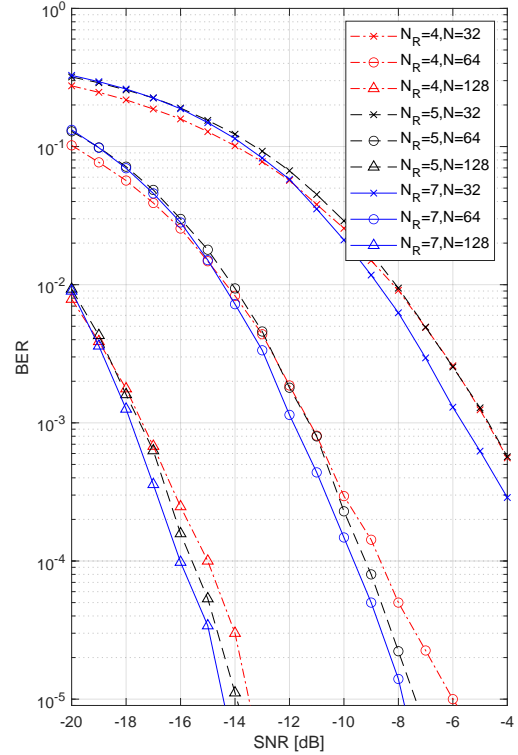


Fig. 2: The BER results of RIS-RGSM with 8APSK and $N_a = 2$ with different conditions in N and N_R .

Firstly, the effect of changing hardware conditions on the proposed RIS-RGSM system is shown in Fig. 2. APSK modulation is adopted with $M_r = 2$, $M_p = 4$ and $M = M_r M_p = 8$. Fix $N_a = 2$ and vary the total number of RIS elements N and the number of receive antennas N_R . To increase diversity, the modulation phases ϕ_l of the second selected antenna all plus a phase offset of $\frac{\pi}{M_p}$, staggered from the received symbols of the first selected antenna. The same operation can be applied for $N_a > 2$. As seen from the given results, when N_R is kept constant, the BER is lower as N increases. Doubling the number of N decreases the SNR required to achieve the same BER by about 6 dB. This is because, with more RIS elements, more reflection paths will be concentrated on a specific selected antenna. Similarly, when N is held constant, BER is lower as N_R increases. It is worth noting that increasing N_R not only makes the BER performance better, but also provides a higher transmission rate R , which is consistent with RIS-RSM in [14]. Moreover, although increasing N and N_R can improve

the BER performance, it comes at the expense of complexity and increased hardware overhead.

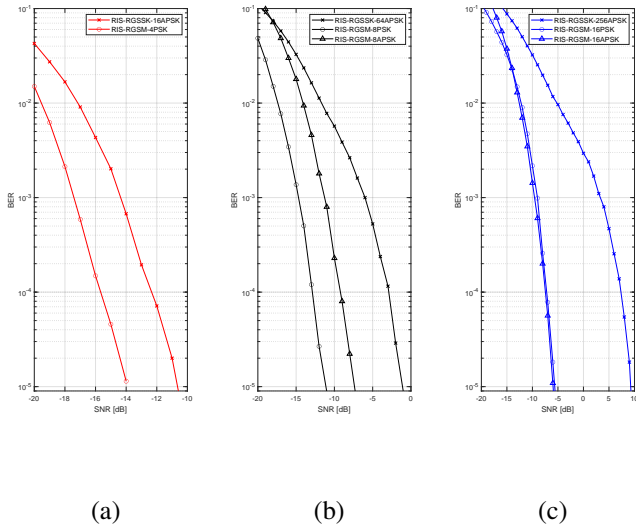


Fig. 3: Comparison of BER results in RIS-RGSM and RIS-RGSSK for $N = 64$, $N_R = 5$, $N_a = 2$ and $R =$ (a) 7, (b) 9, (c) 11 bpcu.

Next, the performance of the proposed RIS-RGSM system is compared with the RIS-RGSSK system at the same transmission rate, as shown in Fig. 3. The transmit antenna of RIS-RGSSK is augmented with the process of sending modulated symbols. For example, in Fig. 3(b), $m_0 = \lfloor \log_2 \binom{N_R}{N_a} \rfloor = \lfloor \log_2 \binom{5}{2} \rfloor = 3$, the modulation order of RIS-RGSSK is $M_{RGSSK} = 64$ and the rate is $R_{RGSSK} = \log_2 M_{RGSSK} + m_0 = 6 + 3 = 9$ bpcu; the modulation order of each selected antenna in RIS-RGSM is $M_{RGSM} = 8$ and the rate is $R_{RGSM} = N_a \log_2 M_{RGSM} + m_0 = 2 \times 3 + 3 = 9$ bpcu. As presented in Fig. 3, when the rates of RIS-RGSM and RIS-RGSSK are equal, the BER performance of RIS-RGSM is better than RIS-RGSSK regardless of whether RIS-RGSM adopts APSK modulation or PSK modulation. To achieve the same BER, for the RIS-RGSM with PSK scheme, the SNR requirement of RIS-RGSM is about 3, 10, and 15 dB lower than RIS-RGSSK when $R = 7, 9$, and 11, respectively; for RIS-RGSM with APSK scheme, the SNR requirement is about 7 and 15 dB lower than RIS-RGSSK when $R = 9$ and 11 bpcu, respectively. The simulation results show the performance superiority of the proposed RIS-RGSM system. The higher the transmission rate, the greater the performance gain of the RIS-RGSM, which benefits from the diversity achieved at multiple selected receive antennas. In addition, in Fig. 3(c), it can be observed that the performance of RIS-RGSM with APSK is better than that with PSK, which leads to the later simulation.

Finally, the performance of RIS-RGSM is compared when APSK and PSK are used respectively, as shown in Fig. 4. It can be found that for low modulation order, that is, $M = 8$, the performance of PSK is better than *APSK*, but when $M = 16$,

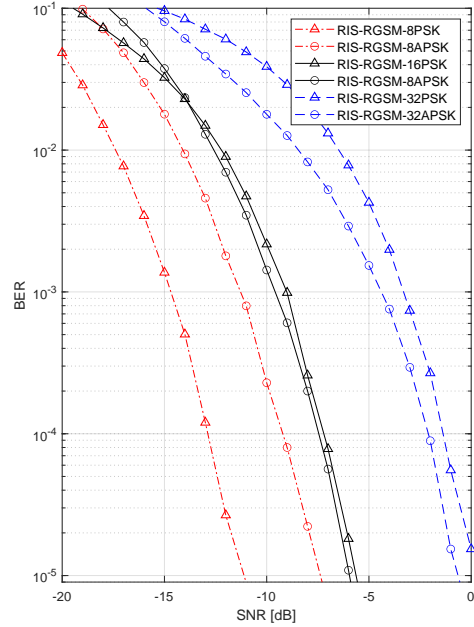


Fig. 4: Comparison results for RIS-RGSM using APSK and PSK respectively, for $N = 64$, $N_R = 5$ and $N_a = 2$.

APSK is slightly better than PSK. The performance gain of APSK is further expanded by increasing the modulation order to $M = 32$. This is because when the modulation order is low, the modulation symbols on the PSK ring are easy to distinguish. In contrast, in the APSK scheme, where the power of the symbols located in the outer ring is constant $\sqrt{E_s}$ according to (7), the symbols located in the inner rings are more difficult to distinguish due to the power limitation. However, when the modulation order is high, the symbols on the single ring of PSK become dense and difficult to distinguish. At this time, APSK can alleviate the problem of dense symbols on the single ring.

V. CONCLUSION

In this paper, the RIS-RGSM system is proposed. Based on the existing RIS-RGSSK model, the additional modulation phases are added to the reflection phases of RIS components to receive different PSK symbols at the selected antennas. Further, control the activation states of RIS components to adjust the amplitude of received symbols so as to receive APSK symbols. Compared with the existing scheme, the proposed RIS-RGSM achieves diversity at the selected antennas, and at the same rate, the RIS-RGSM performs better. In addition, for low modulation orders, RIS-RGSM performs better with PSK, while for high modulation orders, APSK is better. The RIS-RGSM enables more efficient and reliable communication. It will be interesting to research the solution to reduce the demodulation complexity in the future.

ACKNOWLEDGMENT

This paper is supported in part by National Natural Science Foundation of China Program(62371291, 62271316, 62101322), the Fundamental Research Funds for the Central Universities and Shanghai Key Laboratory of Digital Media Processing (STCSM 18DZ2270700). The corresponding author is Yin Xu (e-mail: xuyin@sjtu.edu.cn).

REFERENCES

- [1] L. Chettri and R. Bera, "A Comprehensive Survey on Internet of Things (IoT) Toward 5G Wireless Systems," *IEEE Internet Things J.*, vol. 7, no. 1, pp. 16–32, 2020.
- [2] Y. Wu, L. P. Qian, H. Mao, X. Yang, H. Zhou, and X. Shen, "Optimal Power Allocation and Scheduling for Non-Orthogonal Multiple Access Relay-Assisted Networks," *IEEE Trans. Mobile Comput.*, vol. 17, no. 11, pp. 2591–2606, 2018.
- [3] J. Tang, J. Luo, M. Liu, D. K. C. So, E. Alsusa, G. Chen, K.-K. Wong, and J. A. Chambers, "Energy Efficiency Optimization for NOMA With SWIPT," *IEEE J. Sel. Topics Signal Process.*, vol. 13, no. 3, pp. 452–466, 2019.
- [4] X. Ou, Y. Xu, H. Hong, D. He, Y. Wu, Y. Huang, and W. Zhang, "A drl-based joint scheduling and resource allocation scheme for mixed unicast-broadcast transmission in 5g," *IEEE Transactions on Broadcasting*, vol. 69, no. 3, pp. 661–674, 2023.
- [5] H. Lei, C. Gao, I. S. Ansari, Y. Guo, Y. Zou, G. Pan, and K. A. Qaraqe, "Secrecy Outage Performance of Transmit Antenna Selection for MIMO Underlay Cognitive Radio Systems Over Nakagami- m Channels," *IEEE Trans. Veh. Technol.*, vol. 66, no. 3, pp. 2237–2250, 2017.
- [6] Y. Zhang, W. He, D. He, Y. Xu, Y. Guan, and W. Zhang, "RIS-Aided LDM System: A New Prototype in Broadcasting System," *IEEE Trans. Broadcast.*, vol. 69, no. 1, pp. 224–235, 2023.
- [7] N. S. Perović, L.-N. Tran, M. Di Renzo, and M. F. Flanagan, "Achievable Rate Optimization for MIMO Systems With Reconfigurable Intelligent Surfaces," *IEEE Trans. Wireless Commun.*, vol. 20, no. 6, pp. 3865–3882, 2021.
- [8] R. Y. Mesleh, H. Haas, S. Sinanovic, C. W. Ahn, and S. Yun, "Spatial Modulation," *IEEE Trans. Veh. Technol.*, vol. 57, no. 4, pp. 2228–2241, 2008.
- [9] M. Di Renzo, H. Haas, A. Ghayeb, S. Sugiura, and L. Hanzo, "Spatial Modulation for Generalized MIMO: Challenges, Opportunities, and Implementation," *Proc. IEEE*, vol. 102, no. 1, pp. 56–103, 2014.
- [10] P. Yang, M. Di Renzo, Y. Xiao, S. Li, and L. Hanzo, "Design Guidelines for Spatial Modulation," *IEEE Commun. Surveys Tuts.*, vol. 17, no. 1, pp. 6–26, 2015.
- [11] J. Jeganathan, A. Ghayeb, and L. Szczecinski, "Generalized space shift keying modulation for MIMO channels," in *Proc. IEEE Int. Symp. Pers., Indoor Mobile Radio Commun., Cannes, France*, Sep. 2008, pp. 1–5.
- [12] A. Younis, N. Serafimovski, R. Mesleh, and H. Haas, "Generalised spatial modulation," in *Proc. IEEE Conf. Rec. 44th Asilomar Conf. Signals, Syst. Comput.*, 2010, pp. 1498–1502.
- [13] L.-L. Yang, "Transmitter Preprocessing Aided Spatial Modulation for Multiple-Input Multiple-Output Systems," in *Proc IEEE Veh. Technol. Conf. (Spring)*, 2011, pp. 1–5.
- [14] E. Basar, "Reconfigurable Intelligent Surface-Based Index Modulation: A New Beyond MIMO Paradigm for 6G," *IEEE Trans. Commun.*, vol. 68, no. 5, pp. 3187–3196, 2020.
- [15] A. E. Cambilen, E. Basar, and S. S. Ikki, "On the Performance of RIS-Assisted Space Shift Keying: Ideal and Non-Ideal Transceivers," *IEEE Trans. Commun.*, vol. 70, no. 9, pp. 5799–5810, 2022.
- [16] T. Ma, Y. Xiao, X. Lei, P. Yang, X. Lei, and O. A. Dobre, "Large Intelligent Surface Assisted Wireless Communications With Spatial Modulation and Antenna Selection," *IEEE J. Sel. Areas Commun.*, vol. 38, no. 11, pp. 2562–2574, 2020.
- [17] S. Lin, B. Zheng, G. C. Alexandropoulos, M. Wen, M. D. Renzo, and F. Chen, "Reconfigurable Intelligent Surfaces With Reflection Pattern Modulation: Beamforming Design and Performance Analysis," *IEEE Trans. Wireless Commun.*, vol. 20, no. 2, pp. 741–754, 2021.
- [18] M. H. Dinan, N. S. Perović, and M. F. Flanagan, "RIS-Assisted Receive Quadrature Space-Shift Keying: A New Paradigm and Performance Analysis," *IEEE Trans. Commun.*, vol. 70, no. 10, pp. 6874–6889, 2022.
- [19] M. H. Dinan, M. Di Renzo, and M. F. Flanagan, "RIS-Assisted Receive Quadrature Spatial Modulation with Low-Complexity Greedy Detection," *IEEE Trans. Commun.*, pp. 1–1, 2023.
- [20] C. Zhang, Y. Peng, J. Li, and F. Tong, "An IRS-Aided GSSK Scheme for Wireless Communication System," *IEEE Commun. Lett.*, vol. 26, no. 6, pp. 1398–1402, 2022.
- [21] E. Basar, "Transmission Through Large Intelligent Surfaces: A New Frontier in Wireless Communications," in *Proc. Eur. Conf. Neww. Commun. (EuCNC)*, 2019, pp. 112–117.
- [22] E. Basar, M. Di Renzo, J. De Rosny, M. Debbah, M.-S. Alouini, and R. Zhang, "Wireless Communications Through Reconfigurable Intelligent Surfaces," *IEEE Access*, vol. 7, pp. 116 753–116 773, 2019.